

PERTURBATIVE QCD PHENOMENOLOGY OF ELASTIC *ed* SCATTERING

A. P. Kobushkin¹, Ya. D. Krivenko-Emetov²

¹ *N. N. Bogolyubov Institute for Theoretical Physics, National Academy of Sciences of Ukraine, Kyiv*

² *Institute for Nuclear Research, National Academy of Sciences of Ukraine, Kyiv*

Electron-deuteron elastic scattering data ($A(Q^2)$ and $B(Q^2)$ structure functions and polarization observables t_{20} , t_{21} and t_{22}) are fit with a model that respects asymptotic properties of perturbative QCD (pQCD) at high momentum transfer. The data analysis shows that pQCD starts from $Q^2 = 3,5(\text{GeV}/c)^2$. Predictions for the magnetic structure function $B(Q^2)$ and the polarization observables at high momentum transfer are given.

1. Introduction

In recent few years new data from TJINAF on the *ed* elastic scattering were reported. They include the electric structure function, $A(Q^2)$, measured with high precision up to $Q^2 = 6(\text{GeV}/c)^2$ [1, 2] and tensor polarization observables, t_{20} , t_{21} and t_{22} , up to $Q^2 = 1,7(\text{GeV}/c)^2$ [3].

This data, together with data on the magnetic structure function $B(Q^2)$, [5] restrict the deuteron structure at scales where quark-gluon degrees of freedom are expected to become refrozen. For example, according to optimistic estimations pQCD should start in the deuteron at Q^2 from few $(\text{GeV}/c)^2$ [4]. It is nice that this prediction was confirmed by analysis of TJINAF data on $A(Q^2)$ at $Q^2 > 2 (\text{GeV}/c)^2$ [2].

For further conclusions about quark-gluon degrees of freedom in the deuteron the spin structure of the deuteron at high Q^2 must be also studied. However data on polarization observables, as well as on the $B(Q^2)$, correspond to $Q^2 (\text{GeV}/c)^2$, which is not enough for pQCD. This is a typical intermediate region between nucleon-meson and quark-gluon pictures, where isobar configurations, meson exchange currents and constituent quark degrees of freedom are all important [6].

The purpose of this work is to investigate phenomenologically smooth connection between nucleon-meson and pQCD regions and make predictions for $B(Q^2)$ and polarization observables at higher Q^2 , where pQCD should work. A parametrization which connects this two regions was proposed earlier by one of the authors (A.P.K.) and A. I. Syamtomov [7]. It assumes power fall off of helicity spin amplitudes at asymptotically high Q^2 , which comes from by quark counting rules. A new analysis of the parametrization [7] which includes the recent TJINAF data was provided in [8]. Now we study logarithmic corrections to the power behavior. Such corrections were shown to be important for the structure function $A(Q^2)$ at highest region of TJINAF energy [2].

The paper is organized as follows. In sect. 2 we discuss general structure of helicity amplitudes for the elastic *ed* scattering in light cone frame (LCF) and predictions of pQCD for the helicity amplitudes at high Q^2 . Parametrization of helicity amplitudes which connect smoothly regions of low and high Q^2 is given in sect. 3. Then, in sect. 4 data base and fitting procedure are summarized. Discussions and conclusions are given in sect. 4.

2. Helicity amplitudes and the deuteron formfactors

2.1. Helicity amplitudes

We provide our calculations in the framework of light-cone frame (which is the same as dynamics in infinite momentum frame, IMF). But there exists one serious problem. Indeed, due to gauge invariance, covariance and discrete symmetries only three of the 36 helicity amplitudes (1) are independent. From naive point of view one might think that different sets of the helicity amplitudes

give the same answer to the deuteron formfactors. Nevertheless direct calculations of Grach and Kondratyuk [9] demonstrate that at the light-cone it is not so. Karmanov and Smirnov [10] (see also Karmanov's paper [11]) have shown that this paradox is connected with incompatibility of transformation properties of approximate current and the deuteron wave function used in practical calculations. As a result nonphysical dependence on orientation of light-front plane ω appears which, in turn, leads to addition nonphysical formfactors. Thus addition analysis of how sensible an appropriate choice on the independent helicity amplitudes is of great importance.

2.2. Helicity amplitudes in LCF

The main objects of our analysis are helicity amplitudes of the $\gamma^* + d \rightarrow d$ transition

$$J_{\lambda', \lambda}^{\mu} = \langle p', \lambda' | j^{\mu} | p, \lambda \rangle \quad (1)$$

where p and p' are momenta and λ and λ' are helicities of the deuteron in initial and final states, respectively.

Due to gauge invariance, covariance and discrete symmetries only three of the 36 helicity amplitudes (1) are independent and one can choose different sets of independent helicity amplitudes. Direct calculations, however, [9] demonstrates that it is not so in dynamics at LCF. This phenomena comes from incompatibility of transformation properties of approximate current and the deuteron wave function used in practical calculations [10, 11]. As a result nonphysical dependence on orientation of light-front plane appears. Thus choice of the independent amplitudes becomes of great importance in pQCD calculations where LCF is often used.

First let's define LCF as a limiting reference system where momentum z-projection of the deuteron in initial and final states, p and p' , comes to infinity

$$\begin{aligned} p^{\mu} &= \left(P + \frac{M^2 + p_{\perp}^2}{4P}, \bar{p}_{\perp}, P - \frac{M^2 + p_{\perp}^2}{4P} \right), \\ p'^{\mu} &= \left(P + \frac{M^2 + p_{\perp}^2}{4P}, -\bar{p}_{\perp}, P - \frac{M^2 + p_{\perp}^2}{4P} \right) \end{aligned} \quad (2)$$

with

$$p^+ \equiv p^0 + p^3 = 2P, \quad p'^+ \equiv p'^0 + p'^3 = 2P, \quad P \gg M^2 + \bar{p}_{\perp}^2. \quad (3)$$

(M is the deuteron mass). In this frame momentum of the virtual photon is given by

$$q^{\mu} = (0, -2\bar{p}_{\perp}, 0), \quad \bar{p}_{\perp} = -(\frac{1}{2}Q, 0). \quad (4)$$

In LCF polarization vectors for the deuteron in initial and final states, respectively, read [9]

$$\begin{aligned} \varepsilon^{\mu}(\lambda = \pm 1, p) &= -\sqrt{\frac{1}{2}} \left(\pm \frac{p_{\perp}}{2P}, \pm 1, i, \mp \frac{p_{\perp}}{2P} \right), \\ \varepsilon^{\mu}(\lambda = 0, p) &= \frac{1}{M} \left(P - \frac{M^2 - p_{\perp}^2}{4P}, \bar{p}_{\perp}, P + \frac{M^2 - p_{\perp}^2}{4P} \right), \\ \varepsilon^{\mu}(\lambda' = \pm 1, p') &= -\sqrt{\frac{1}{2}} \left(\mp \frac{p_{\perp}}{2P}, \pm 1, i, \pm \frac{p_{\perp}}{2P} \right), \\ \varepsilon^{\mu}(\lambda' = 0, p') &= \frac{1}{M} \left(P - \frac{M^2 - p_{\perp}^2}{4P}, -\bar{p}_{\perp}, P - \frac{M^2 - p_{\perp}^2}{4P} \right). \end{aligned} \quad (5)$$

Using the standard expression for the current matrix element

$$\begin{aligned}
 J_{\lambda, \lambda'}^{\mu} = & -\{G_1(Q^2)\varepsilon^*(\lambda', p')\varepsilon(\lambda, p)(p + p') + \\
 & + G_2(Q^2)[\varepsilon^{\mu}(\lambda, p)(\varepsilon^*(\lambda', p')q) - \varepsilon^{*\mu}(\lambda', p')(\varepsilon(\lambda, p)q)] - \\
 & - G_3(Q^2)(p + p')^{\mu} \frac{(\varepsilon^*(\lambda', p')q)(\varepsilon(\lambda, p)q)}{2M^2}\}
 \end{aligned} \quad (6)$$

one gets for the plus-component of the e.-m. current matrix elements

$$J_{00}^+ = p^+ \{2(1 - 2\eta)G_1 + 4\eta G_2 - 4\eta^2 G_3\}, \quad (7)$$

$$J_{10}^+ = p^+ \{2\sqrt{2\eta}G_1 - \sqrt{2\eta}G_2 + 2\sqrt{2\eta}\eta G_3\}, \quad (8)$$

$$J_{1-1}^+ = -p^+ \{2\eta G_3\}, \quad (9)$$

$$J_{11}^+ = p^+ \{2G_1 + 2\eta G_3\}. \quad (10)$$

where $J_{\lambda\lambda'}^+ \equiv J_{\lambda\lambda'}^0 + J_{\lambda\lambda'}^3$. It is nothing to show that they satisfy the so-called angular condition

$$(1 + 2\eta)J_{11}^+ + J_{1-1}^+ - 2\sqrt{2\eta}J_{10}^+ - J_{00}^+ = 0 \quad (11)$$

and thus there are only three independent helicity amplitudes among the J_{11}^+ , J_{1-1}^+ , J_{10}^+ , J_{00}^+ [9, 12].

Alternatively the angular condition teaches us that even at the pQCD extreme there appears (through dimensionless ratio $\eta = \frac{Q^2}{4M^2}$) an additional scale parameter $4M^2$, apart from the pQCD parameter $\Lambda_{QCD}^2 \ll Q^2 \leq 4M^2$.

2.3. The deuteron formfactors

The charge, $G_c(Q^2)$, magnetic, $G_m(Q^2)$, and quadrupole, $G_Q(Q^2)$, formfactors are connected with formfactors $G_1(Q^2)$, $G_2(Q^2)$ and $G_3(Q^2)$ as follows

$$\begin{aligned}
 G_Q &= G_1 - G_2 + (1 + \eta)G_3, \\
 G_c &= G_1 + \frac{2}{3}\eta G_Q,
 \end{aligned} \quad (12)$$

$$G_m = G_2.$$

Using (10) one expresses the $G_c(Q^2)$, $G_m(Q^2)$ and $G_Q(Q^2)$ in terms of any three helicity amplitudes $J_{\lambda\lambda'}^+$, for example

$$\begin{aligned}
 G_c &= \frac{1}{2P(2\eta + 1)} \left[\frac{3 - 2\eta}{6} J_{00}^+ + \frac{8}{3} \sqrt{\frac{\eta}{2}} J_{10}^+ + \frac{2\eta - 1}{3} J_{1-1}^+ \right], \\
 G_m &= \frac{1}{2P(2\eta + 1)} \left[J_{00}^+ + \frac{(2\eta - 1)}{\sqrt{2\eta}} J_{10}^+ - J_{1-1}^+ \right],
 \end{aligned}$$

$$G_q = \frac{1}{2P(2\eta+1)} \left[-\frac{1}{2} J_{00}^+ + \sqrt{\frac{1}{2\eta}} J_{10}^+ - \frac{\eta+1}{2\eta} J_{1-1}^+ \right]. \quad (13)$$

In turn, the $A(Q^2)$ and $B(Q^2)$ structure functions and $t_{2i}(\theta, Q^2)$ polarization's read

$$A = G_c^2 + \frac{2}{3} \eta G_m^2 + \frac{8}{9} \eta^2 G_Q^2, \quad (14)$$

$$B = \frac{4}{3} \eta(1+\eta) G_m^2, \quad (15)$$

$$t_{20} = \frac{-\left(\frac{8}{9} \eta^2 G_Q^2 + \frac{8}{9} \eta G_c G_Q + \frac{2}{3} \eta G_m^2 \left[\frac{1}{2} + (1+\eta) \operatorname{tg}^2\left(\frac{\theta}{2}\right)\right]\right)}{\sqrt{2} [A^2 + B^2 \operatorname{tg}^2\left(\frac{\theta}{2}\right)]}, \quad (16)$$

$$t_{21} = \frac{2\eta(\eta + \eta^2 \sin^2\left(\frac{\theta}{2}\right))^{1/2} G_m G_Q}{\sqrt{3} [A^2 + B^2 \operatorname{tg}^2\left(\frac{\theta}{2}\right)] \cos\left(\frac{\theta}{2}\right)}, \quad (17)$$

$$t_{22} = \frac{-G_m^2}{2\sqrt{3} [A^2 + B^2 \operatorname{tg}^2\left(\frac{\theta}{2}\right)]}. \quad (18)$$

In the present paper we prefer to use the set $J_{1,1}^+, J_{1,-1}^+$ and $J_{1,0}^+$. In this case the formfactors $G_c(Q^2)$, $G_m(Q^2)$ and $G_q(Q^2)$ are expressed as

$$G_c = \frac{1}{4P} \left[J_{11}^+ + \frac{1}{3} \sqrt{2\eta} J_{10}^+ + \frac{1}{3} J_{1-1}^+ \right], \quad (19)$$

$$G_m = \frac{1}{4P} \left[J_{11}^+ - \frac{1}{\sqrt{2\eta}} J_{10}^+ \right], \quad (20)$$

$$G_q = \frac{1}{4P} \left[\sqrt{\frac{1}{2\eta}} J_{10}^+ - \frac{1}{\eta} J_{1-1}^+ \right]. \quad (21)$$

2.4. Ambiguities in the IMF

The main problem is that the angular condition (11) is usually violated [7] in the IMF calculations and choice of independent helicity amplitudes become of great importance. Links between the different choices in the IMF calculations are given in [9]. For example it was shown that in the light-cone dynamics the matrix elements (1) become dependent on the ω . If it is fixed as in (3) the helicity amplitudes (7) and (8) are transformed to

$$J_{00}^+(IMF) = J_{00}^+ - 2\eta B_6 + (B_5 + B_7), \quad (22)$$

$$J_{10}^+(IMF) = J_{10}^+ + \sqrt{\frac{\eta}{2}} B_6. \quad (23)$$

The amplitudes (10) and (9) are not changed. The formfactors B_i are nonphysical and must vanish in exact theory (where the e.m. current and equation for the relativistic deuteron wave functions are self-consistent) [Definition of the nonphysical formfactors B_i is given in [8, 9]]. But

in any approximate theory, like asymptotic QCD, they are not zero and must be excluded from the final results.

2.5. pQCD predictions for the helicity amplitudes

From pQCD arguments one gets very simple rules to determine power behavior of the helicity amplitudes J_{00}^+ , J_{10}^+ and J_{1-1}^+ [13, 14]. For example it gives that the amplitude J_{00}^+ is a leading amplitude with asymptotic fall off (neglecting logarithmic corrections)

$$J_{00}^+ \sim \left(\frac{\Lambda_{QCD}}{Q} \right)^{10}. \quad (24)$$

It was also argued that in the IMF the helicity flip amplitudes $J_{1,0}^+$ and $J_{1,-1}^+$ are suppressed as [15]

$$\frac{J_{10}^+}{J_{00}^+} \sim \left(\frac{\Lambda_{QCD}}{Q} \right), \quad \frac{J_{1-1}^+}{J_{00}^+} \sim \left(\frac{\Lambda_{QCD}}{Q} \right)^2. \quad (25)$$

The similar considerations give that

$$J_{11}^+ \sim J_{1-1}^+ \sim \left(\frac{\Lambda_{QCD}}{Q} \right)^2 J_{00}^+, \quad (26)$$

which agrees with the angular condition (11) at extreme high Q^2 -region, $Q^2 \gg 4M^2$.

In our analysis, following arguments of Ref.[15], we consider the set J_{00}^+ , J_{10}^+ and J_{1-1}^+ as a main amplitudes, which behavior (24) and (26) is regulated in the intermediate region only by the Λ_{QCD} . In turn, the amplitude J_{11}^+ must be determined from the angular condition (11) and thus it depends on the two scale parameters, Λ_{QCD} and $4M^2$.

3. Parametrization of helicity transition amplitudes

Following the idea of reduced nuclear amplitudes in the QCD [17], we define the reduced helicity transition amplitudes g_{00} , g_{0+} and g_{+-} as follow

$$\frac{1}{4P} J_{\lambda',\lambda}^+(Q^2) = G^2 \left(\frac{Q^2}{4} \right) g_{\lambda',\lambda}^+(Q^2), \quad (27)$$

where $G(Q^2)$ is a three-quark-cluster (nucleon) formfactor. For the $G(Q^2)$ we assume dipole behavior $G(Q^2) = [1 + \frac{Q^2}{\mu^2 (GeV/c)^2}]^{-2}$, but due to medium effects the parameter μ^2 should be different from that for a free nucleon $0.71 (GeV/c)^2$.

We consider separately two kinematical regions, large Q^2 region, $Q^2 > Q_0^2$, and low Q^2 region, $Q^2 < Q_0^2$. The parameter Q_0^2 is estimated to be of order of few $(GeV/c)^2$. Its exact value will be determined from fit to experimental data.

For the Q^2 reduced transition amplitudes we use the asymptotic prediction of the pQCD

$$\begin{aligned}
g_{00}^{+(asy)} &= \frac{N_1(\Lambda_{QD}^2)}{Q^2} f(Q/\Lambda_{QD}^2), \quad g_{0+}^{+(asy)} = \frac{N_2(\Lambda_{QD}^2)}{Q^3} f(Q/\Lambda_{QD}^2), \\
g_{+-}^{+(asy)} &= \frac{N_3(\Lambda_{QD}^2)}{Q^4} f(Q/\Lambda_{QD}^2)
\end{aligned} \tag{28}$$

where the factor $f(Q^2)$ takes into account logarithmic corrections

$$f(Q^2/\Lambda_{QCD}^2) = \frac{[\alpha_s(Q^2)]^5 (\lg(Q^2/\Lambda_{QCD}^2))^{-2\gamma^d}}{[\lg(Q^2/4\Lambda_{QCD}^2)]^{-4\gamma^N}} \tag{29}$$

and γ^d and γ^N are leading anomalous dimensions for the deuteron and the nucleon, respectively. They are given by

$$\gamma^d = \frac{6C_F}{5\beta}, \quad \gamma^N = \frac{C_F}{2\beta}. \tag{30}$$

After symmetryzations the anomalous dimensions are given by [36], [37]

$$\gamma_{real}^d = \frac{3C_F}{4\beta}, \quad \gamma^N = \frac{C_F}{2\beta}, \tag{31}$$

where $C_F = (n_c^2 - 1)/(2n_c)$, $\beta = 11 - \frac{2}{3}n_f$, $n_c = 3$ - is number of quark colors and $n_f = 3$ is the number of flavors, $\alpha_s(Q^2) = \frac{4\pi}{\beta \lg Q^2/\Lambda_{QCD}^2}$ is the running quark-gluon coupling [4]. Of course, the anomalous dimensions depend also on helicities, but we ignored this dependence, because, according [36]

$$\begin{aligned}
\delta J_{real}^{\max} &\approx \alpha_s^5(Q^2) \frac{N}{Q^{10}} \ln^{C_f/2\beta}(Q^2/\Lambda_{QCD}^2) \left\{ 1 - \frac{N}{Q^2} \ln^{-C_f/4\beta}(Q^2/\Lambda_{QCD}^2) \right\}, \\
\delta J_{over}^{\max} &\approx \alpha_s^5(Q^2) \frac{N}{Q^{10}} \ln^{C_f/2\beta}(Q^2/\Lambda_{QCD}^2) \left\{ 1 - \frac{N}{Q^2} \right\}, \\
\delta J_{real}^{\max} - \delta J_{over}^{\max} &\approx \alpha_s^5(Q^2) \frac{N}{Q^{12}} \ln^{C_f/2\beta}(Q^2) \left\{ \ln^{-C_f/4\beta}(Q^2) - 1 \right\}.
\end{aligned} \tag{32}$$

The constants N_1 , N_2 and N_3 introduced in (28) cannot be calculated from the pQCD. We will determine them from smooth connection with the reduced transition amplitudes at $Q^2 \leq Q_0^2$. At $Q^2 \leq Q_0^2$ the following parametrization for the reduced amplitudes is assumed

$$\begin{aligned}
\tilde{g}_{00}^+ &= \sum_{n=1}^N \frac{a_n}{Q^2 + \alpha_n^2}, \quad \tilde{g}_{0+}^+ = Q \sum_{n=1}^N \frac{b_n}{Q + \alpha_n}, \\
\tilde{g}_{+-}^+ &= Q^2 \sum_{n=1}^N \frac{c_n}{Q^2 + \alpha_n^2},
\end{aligned} \tag{33}$$

where $\alpha_n^2 = \alpha_0^2 + nm_0^2$. To satisfy normalization conditions for the reduced amplitudes at Q^2 one has to improve the following constrains on the coefficients a_n , b_n and c_n (see, e.q. [7]):

$$\sum_{n=1}^N \frac{a_n}{\alpha_n^2} = 1, \quad \sum_{n=1}^N \frac{b_n}{\alpha_n^2} = \frac{2 - \mu_d}{2\sqrt{2}M}, \quad \sum_{n=1}^N \frac{c_n}{\alpha_n^2} = \frac{1 - \mu_d - Q_d}{2M^2} \quad (34)$$

on the coefficients a_n , b_n and c_n to demand formfactor normalization at $Q^2 = 0$. In Eqs. (34) $\mu_d = 0.857406 M / m_p$ is the deuteron magnetic moment in “deuteron magnetons” and $Q_d = 25,84$ is the deuteron quadrupole momentum in M^2/e .

The coefficients N_1 , N_2 and N_3 appearing in (28) of the reduced helicity flip amplitudes in the asymptotic region are determined from smooth connection parametrization at the point $Q^2 = Q_0^2$:

$$g^{+(asy)}_{ij}(Q_0^2) = \tilde{g}^+_{ij}(Q_0^2), \quad \frac{\partial^2 g^{+(asy)}_{00}}{\partial Q^2} = \frac{\partial^2 \tilde{g}^+_{00}}{\partial Q^2}, \quad (35)$$

$$\frac{\partial g^{+(asy)}_{0+}}{\partial Q} = \frac{\partial \tilde{g}^+_{0+}}{\partial Q}, \quad \frac{\partial^2 g^{+(asy)}_{+-}}{\partial Q^2} = \frac{\partial^2 \tilde{g}^+_{+-}}{\partial Q^2}.$$

4. Data base and fitting parameters

In our fit we use the following data: for $A(Q^2)$ from [1, 2, 18, 20 - 25], for $B(Q^2)$ from [5, 20, 21, 26, 27] and polarization observables t_{20} from [3, 29 - 32, 34] and t_{22} , t_{21} from [3, 31]. But it must

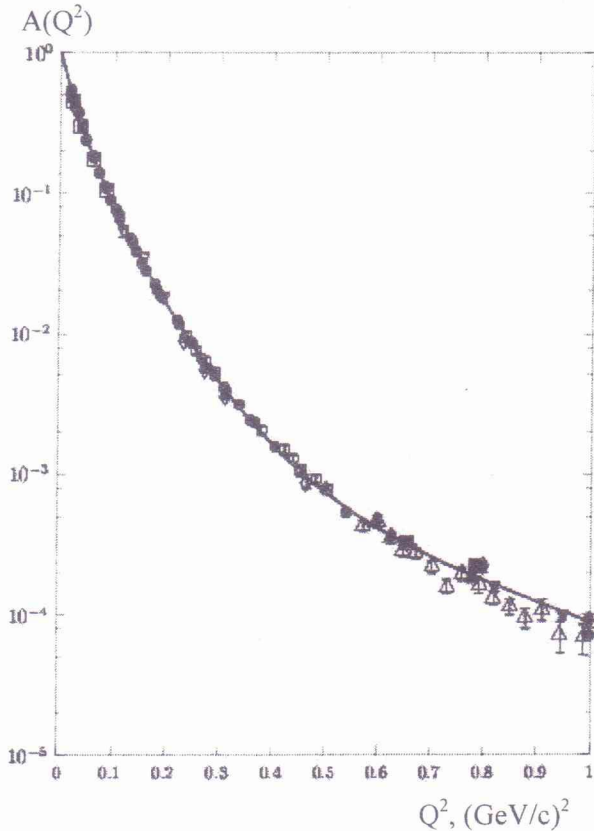


Fig. 1. Comparison of the model fit with data for $A(Q^2)$ at $Q^2 < 1$ $(\text{GeV}/c)^2$.

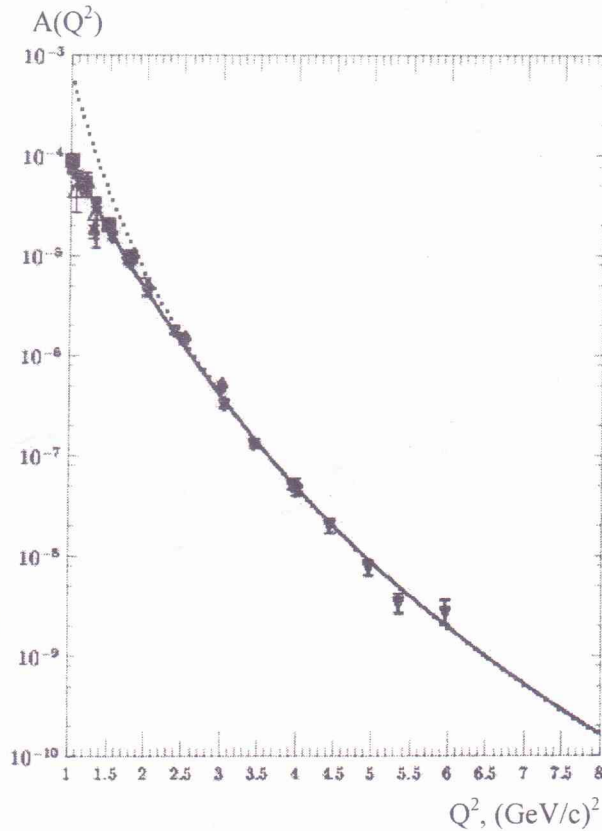


Fig. 2. Comparison of the model fit [solid] with data for $A(Q^2)$ at $Q^2 > 1$ $(\text{GeV}/c)^2$. Dotted line is asymptotic behavior given by (28) and (30) extrapolated to lower transfer momentum.

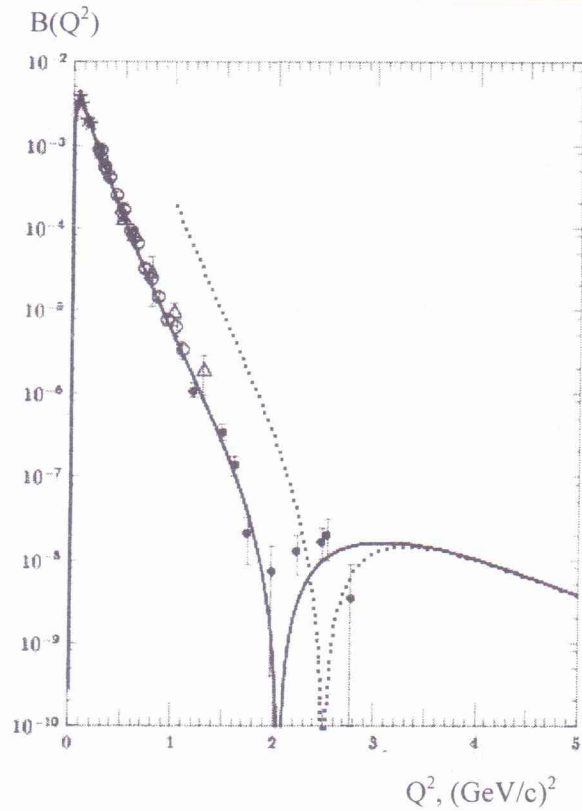


Fig. 3. Comparison of the model fit [solid] with data for $B(Q^2)$. Dotted line is asymptotic behavior given by (28) extrapolated to lower transfer momentum.

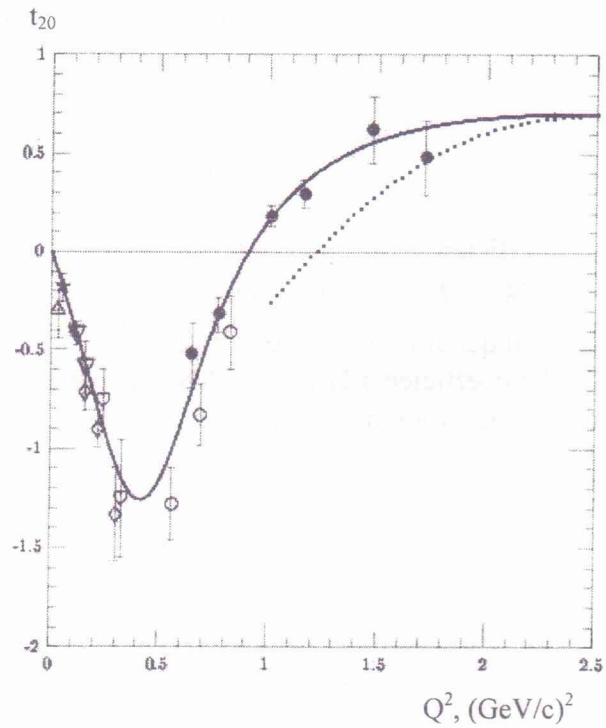


Fig. 4. Comparison of the model fit [solid] with data for t_{20} . Dotted line is asymptotic behavior given by (28) extrapolated to lower transfer momentum.

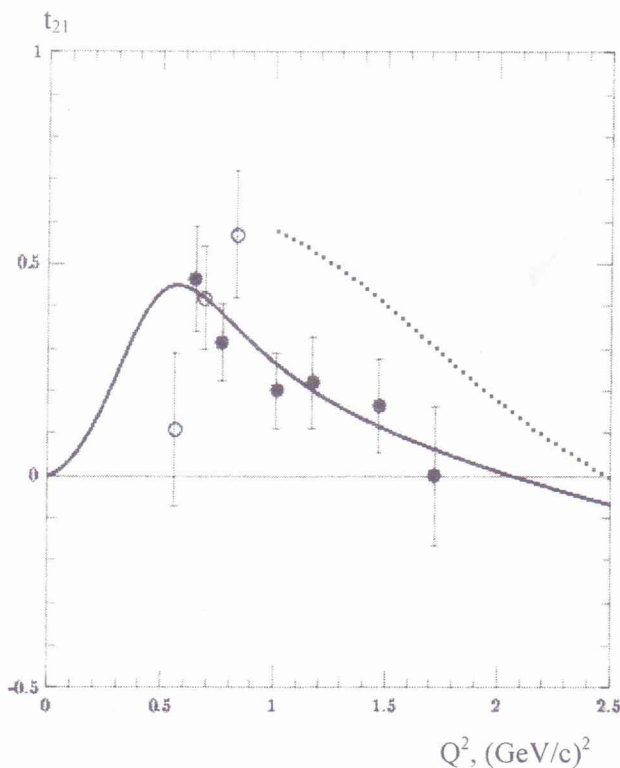


Fig. 5. Comparison of the model fit [solid] with data for t_{21} . Dotted line is asymptotic behavior given by (28) extrapolated to lower transfer momentum.

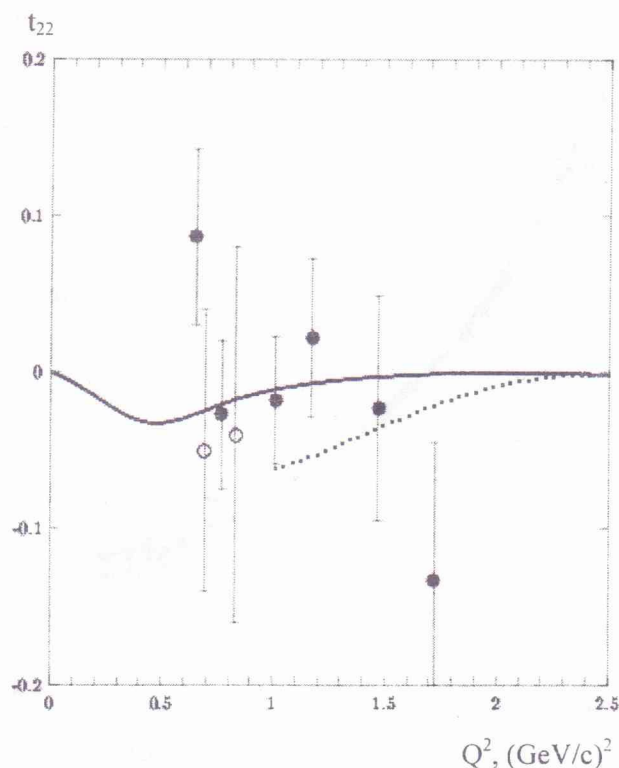


Fig. 6. Comparison of the model fit [solid] with data for $|G_c(Q^2)|$ [8]. For the last two points the two solutions (filled and open points) are shown, see [8]. Dotted line is asymptotic behavior given by (28) extrapolated to lower transfer momentum.

be noted that due to large errors t_{22}, t_{21} data are practically not informative for the fit. Data for A from [27] are in sharp contradiction with all the world data set and therefore were omitted from the fit. We also do not include in the data base results from [35] because they have large errors and practically do not change the obtained results. Data [23] are somewhat lower than the world data, but due to large their uncertainties the fit is insensitive to this data. Data for the B structure function were normalized, if necessary, to our convention of the magnetic form factor.

Q_{QCD}^2 was considered as a parameter of the model, but the QCD cutoff parameter Λ_{QCD} was fixed at 220 MeV. In (33) and (34) we chose $N = 4$, so that the model has 10 independent fit parameters. The fit parameters summarized in Table 1 [38] were obtained with $\chi^2 = 399$ for 200 data points.

5. Discussion and summary

Figs. 1 and 2 display comparison of the model with $A(Q^2)$ data. To show how far experimental data are from pQCD results in preasymptotic region we continue asymptotic behavior given by (28) to region lower than Q_{QCD}^2 (dotted line in fig. 2 and figs. 3 - 7). One concludes that for $A(Q^2)$ pQCD works from Q^2 -region between 1 and 2 $(\text{GeV}/c)^2$. Comparison with data for $B(Q^2)$ and the polarization observables are given in figs. 3 - 5. One sees that for the magnetic form factor pQCD should start from Q^2 between 2 and 3 $(\text{GeV}/c)^2$, but for the polarization observable it should start somewhat earlier, near 2 $(\text{GeV}/c)^2$.

Fig. 7 shows results for the charge and quadrupole form factors, $G_c(Q^2)$ and $G_q(Q^2)$.

In summary, we give a parameterization of the deuteron form factors up to $Q^2 = 6 (\text{GeV}/c)^2$. Asymptotic behavior of the form factors is dictated by quark counting rules and pQCD helicity rules and therefore one may hope that this parameterization can be extrapolated for higher transferred momentum. For example, the model predicts behavior of the magnetic structure function, $B(Q^2)$, at $Q^2 \geq 2.5 (\text{GeV}/c)^2$ which can be studied in future experiments.

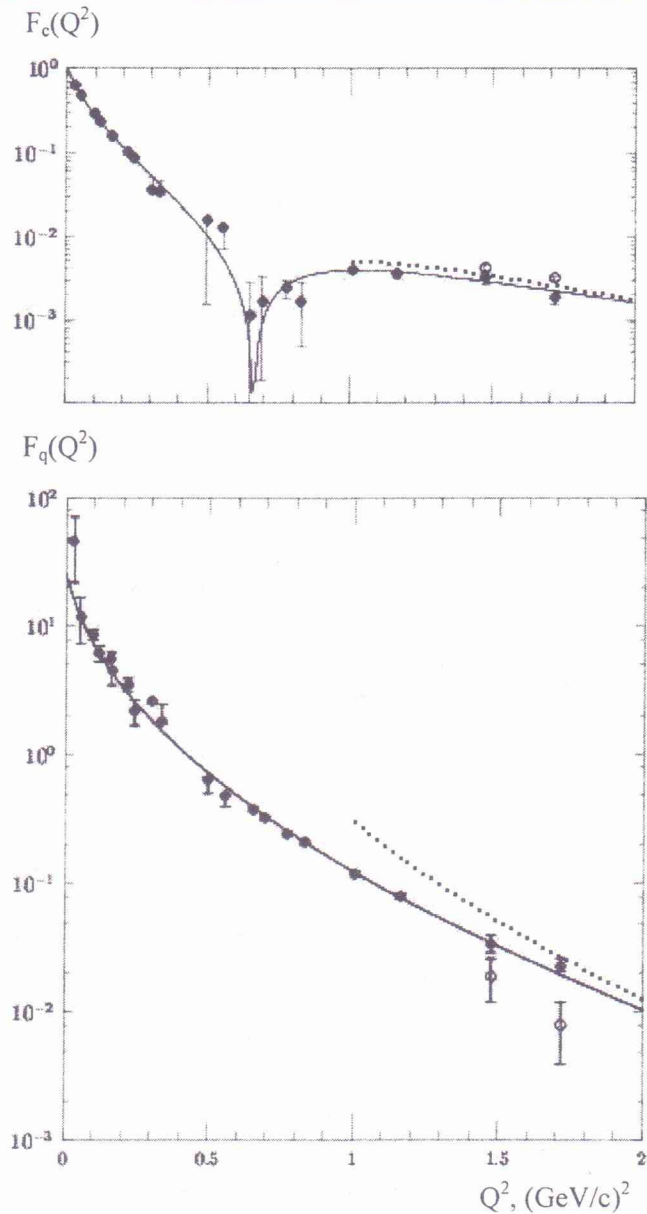


Fig. 7. Comparison of the model fit [solid] with data for $G_Q(Q^2)$ [8]. For the last two points the two solutions (filled and open points) are shown, see [8]. Dotted line is asymptotic behavior given by (28) extrapolated to lower transfer momentum.

Acknowledgments

We thank M. Garcon, G. G. Petratos and E. A. Strokovsky for number of helpful discussions.

One of the authors (A. P. K.) acknowledges the hospitality of RCNP, where this work was carried out with Center of Excellence grant from the Ministry of Education, Culture, Sports, Science and Technology (Monbu-Kagaku-sho), Japan.

Ya. D. K.-E. acknowledges the financial support from the Applied Physics Department of Kyiv National Technical University, Project N2700/162. He also thanks Prof. V. M. Kolomiets for the assistance.

REFERENCES

1. *Alexa L.C., Anderson B.D., Aniol K.A. et al. // Phys. Rev. Lett. - 1999. - Vol. 82. - P. 82. - P. 1374.*
2. *Abbott D., Ahmidouch A., Anklin H. et al. // Ibid. - P. 1379.*
3. *Abbott D., Ahmidouch A., Anklin H. et al. // Ibid. - 2000. - Vol. 84. - P. 5053.*
4. *Brodsky S.J., Ji C.-R., Lepage G.P. // Ibid. - 1983. - Vol. 51. P. 83.*
5. *Bosted P.E., Breton V., Borel H. et al. // Phys. Rev. C - 1990. - Vol. 42. - P. 38.*
6. *Lomon E. // nucl-th/0002026. - 2000; Phys. Rev. C - 2001. - Vol. 64. - P. 035204.*
7. *Kobushkin A.P., Syptomov A.I. // Phys. Atom. Nucl. - 1995. - Vol. 58. - P. 1477.*
8. *Abbott D., Ahmidouch A., Anklin H. et al. // Eur. Phys. J. A - 2000. - Vol. 7. - P. 421.*
9. *Grach I.L., Kondratyuk L.A. // Sov. J. Nucl. Phys. - 1984. - Vol. 39. - P. 198.*
10. *Karmanov V.A., Smirnov A.V. // Nucl. Phys. A - Vol. 1992. - Vol. 546. - P. 691.*
11. *Karmanov V.A. // Ibid. - 1996. - Vol. 608. - P. 316.*
12. *Chung P.L., Coester F., Keister B.D., Polyzou W.N. // Phys. Rev. C - 1988. - Vol. 37. - P. 2000.*
13. *Vainshtein A.I., Zakharov V.I. // Phys. Lett. B - 1978. - Vol. 72. - P. 368.*
14. *Carlson C., Gross F. // Phys. Rev. Lett. - 1984. - Vol. 53. - P. 127.*
15. *Brodsky S.J., Hiller J.R. // Phys. Rev. D - 1992. - Vol. 46. P. 2141.*
16. *Kobushkin A.P., Syantomov A.I. // Ibid. - 1994. - Vol. 49. - P. 1637.*
17. *Brodsky S.J., Chertok B.T. // Phys. Rev. Lett. - 1976. - Vol. 37. - P. 269; Phys. Rev. D - 1976. - Vol. 14. - P. 3003.*
18. *Arnold R.G., Chertok B.T., Jordan C.L. et al. // Ibid. - 1975. - Vol. 35. - P. 776.*
19. *Benaksas D., Drickey D., Frerejacque D. et al. // Phys. Rev. - 1966. - Vol. 148. - P. 1327.*
20. *Buchanan C.D., Yeadrian R. // Phys. Rev. Lett. - 1965. - Vol. 15. - P. 303.*
21. *Cramer R., Haghund R.F., Beylkin G. et al. // Z. Phys. C - 1985. - Vol. 29. - P. 513.*
22. *Drikley D.J., Hand L.N. // Phys. Rev. Lett. - 1962. - Vol. 9. - P. 521.*
23. *Elias J.E., Fridman J.J., Hartmann G.C. et al. // Phys. Rev. 1969. - Vol. 177. - P. 521.*
24. *Gaster S. et al. // Nucl. Phys. B - 1971. - Vol. 32. - P. 221.*
25. *Plachkov S. et al. // Nucl. Phys. A - 1990. - Vol. 510. - P. 740.*
26. *Aufert S. et al. // Phys. Rev. Lett. - 1975. - Vol. 54. - P. 776.*
27. *Simon G.G., Schmitt Ch., Walter V.H. et al. // Nucl. Phys. A - 1981. - Vol. 364. - P. 285.*
28. *Bouwhuis M., Alarcon R., Botto T. et al. // Phys. Rev. Lett. - 1999. - Vol. 82. - P. 3755.*
29. *Dmitriev V.F., Nikolaenko D.M., Shatunov Yu.M. et al. // Phys. Lett. - 1985. - Vol. 157B. - P. 143.*
30. *Ferro-Luzzi M., Bouwhuis M., Paschiev E. et al. // Phys. Rev. Lett. - 1996. - Vol. 77. - P. 2630.*
31. *Garcon M., Arvieux J., Gameron J.M. et al. // Phys. Rev. C - 1994. - Vol. 49. - P. 2516.*
32. *Gilman R., Holtet R.J., Mordechai S. et al. // Phys. Rev. Lett. - 1990. - Vol. 65. - P. 1733.*
33. *Schulze M.E., Beck D., Gilad S. et al. // Ibid. - 1984. - Vol. 52. - P. 597.*
34. *Voitsekhovskii B.B. et al. // JETP Lett. - 1986. - Vol. 43. - P. 733.*
35. *Akimov Yu.K. et al. // Yad Fiz. - 1979. - Vol. 29. - P. 649.*
36. *Ji C.-R., Brodsky S. // Phys. Rev. D - 1986. - Vol. 34, No. 5.*
37. *Brodsky S., Ji C.-R. // Ibid - Vol. 33, No. 9.*
38. *Kobushkin A.P., Krivenko Ya.D. // nucl-th/0112009. - 2002.*

**ФЕНОМЕНОЛОГІЯ ПРУЖНОГО *ed* РОЗСІЯННЯ В ПРЕДСТАВЛЕННІ
ПЕРТУРБАТИВНОЇ КХД****А. П. Кобушкін, Я. Д. Кривенко-Єметов**

Дані по пружному електрон-дейтронному розсіянню (для $A(Q^2)$ та $B(Q^2)$ структурних функцій і тензорів поляризації t_{20} , t_{21} та t_{22}) досліджувались у моделі, яка при великих переданих імпульсах узгоджується з уявленнями пертурбативної КХД (пКХД). Аналіз даних показав, що пКХД непогано узгоджується з експериментом приблизно з $Q^2 = 3,5(GeV/c)^2$.

**ФЕНОМЕНОЛОГІЯ УПРУГОГО *ed* РАССЕЯНИЯ В ПРЕДСТАВЛЕНИИ
ПЕРТУРБАТИВНОЙ КХД****А. П. Кобушкин, Я. Д. Кривенко-Еметов**

Данные по упругому электрон-дейтронному рассеянию (для $A(Q^2)$ и $B(Q^2)$ структурных функций и тензоров поляризации t_{20} , t_{21} и t_{22}) изучались в модели, которая при больших переданных импульсах согласуется с предсказаниями пертурбативной КХД (пКХД). Анализ данных показывает, что пКХД неплохо согласуется с экспериментом примерно с $Q^2 = 3,5(GeV/c)^2$.

Received 07.07.03,
revised - 17.12.03.